CEBAF PROPOSAL COVER SHEET

This Proposal must be mailed to:

CEBAF
Scientific Director's Office
12000 Jefferson Avenue
Newport News, VA 23606

and received on or before 1 October 1991.

A. TITLE: A Precision Measurement of A_e in $p(\vec{e},e'p)\pi^0$

B. CONTACT PERSON: Dave Mack

ADDRESS, PHONE, AND ELECTRONIC MAIL ADDRESS:

CEBAF MS-12H
12000 Jefferson Ave.
Newport News, VA 23606
MACK@CEBAF (804) 249-7442

C. IS THIS PROPOSAL BASED ON A PREVIOUSLY SUBMITTED PROPOSAL OR LETTER OF INTENT?

☐ YES ☑ NO

IF YES, TITLE OF PREVIOUSLY SUBMITTED PROPOSAL OR LETTER OF INTENT:

****

(CEBAF USE ONLY)

Receipt Date 1 OCT 91

Log Number Assigned PR 91-019

By [redacted]

CEBAF Proposal:

A Precision Measurement of A_e in $p(\vec{e}, e'p)\pi^o$

D. Mack (Spokesperson), D. Abbott*, R. Carlini, Y. Chen,
J. Napolitano, A. Saha, W. Vulcan, S. Wood
Physics Division, CEBAF

O.K. Baker
Physics Department, Hampton University,
and Physics Division, CEBAF

A. Klein
Old Dominion University

B. Mayes, L. Pinsky, L. Tang
Physics Department, University of Houston

* *Also affiliated with the Physics Department,*
College of William and Mary.

Abstract

We propose a precision measurement of A_e, the electron helicity flip asymmetry, in the reaction $p(\vec{e}, e'p)\pi^0$ over the $\Delta(1232)$ resonance at Q^2 of .3 and .4 $(GeV/c)^2$. The observable A_e is interesting because it is sensitive to the G_C (charge) form factor in the N$\rightarrow$ Δ transition, and a non-zero value for this form factor would suggest nucleon or Δ deformation. A_e is also of interest because its relatively simple multipole structure may simplify the treatment of Born backgrounds. We show this important out-of-plane measurement is possible due to the large vertical acceptance of the HMS-SOS spectrometer system for $Q^2 \geq .3$ $(GeV/c)^2$.

1 Introduction

1.1 Physics Motivation

The $\Delta(1232)$ resonance has a very special place in N* physics. It is the least massive baryon resonance, the most strongly excited at low Q^2, and it is relatively well separated from other resonances. Its first-order quark structure, three spin-aligned quarks in relative s-states, is well known. Because effects of the Δ are ubiquitous in intermediate energy nuclear physics, Hamiltonian models exist which incorporate the $\Delta \rightarrow N\pi$ transition and the effects of off-shell pion rescattering. Measurements are simplified by the fact that the Δ tends to decay into two-body final states: N+π (99.4%) or N+γ (.6%). For these reasons, the $\Delta(1232)$ is an ideal candidate for modern precision studies of baryon structure which go beyond the first order quark model.

Isgur and collaborators [1] have predicted that both the N and Δ have small d-wave components due to quark-quark hyperfine interactions. These components would permit a very small E2 amplitude (E2/M1 $\simeq$ .007) in the $\Delta \rightarrow N\gamma$ transition. (C2 amplitudes were not estimated because only $\Delta \rightarrow N\gamma$ *decays* were considered.) In a nonrelativistic model with no hyperfine interactions, the quark wave functions for the N and Δ are L=0 and so cannot be coupled by the L=2 quadrupole operator. The transition is then purely M1 [2]. Complicating this tale is the observation of Bienkowska *et al.* [3] that the use of relativistic wave functions yields E2/M1 = -.002 even in the absense of tensor forces. Isgur *et al.* also mention a number of apparent successes of the quark-quark hyperfine interaction, and propose the search for E2 admixtures as a way to rule out an alternative explanation in terms of spin-orbit effects.

There is also evidence from bag models of non-strange baryons that at least some baryons may be deformed. Viollier *et al.* [4] found that the one-gluon exchange interaction caused the Δ bag to become deformed as much as 30%. Meanwhile, minimum energy was obtained for the nucleon bag when it was given zero deformation. Murphy and Bhaduri [5] have investigated deformation as a means of improving the description of higher mass resonances such as the N(1440) and the N(1710), while maintaining the successes of the spherical model of Isgur and Karl. [6]

Many researchers believe that possible deformation of the nucleon and Δ is a question of fundamental importance. There are other pieces of circumstancial evidence which suggest

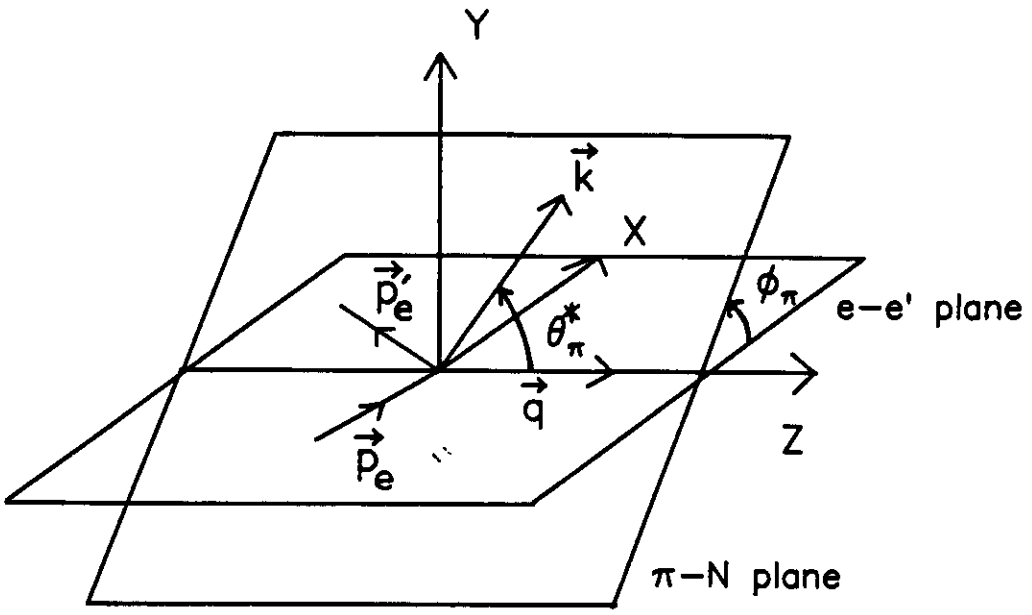

Figure 1: Definition of kinematic variables in electroproduction. Of particular importance in our discussion are the pion polar angle θ_π with respect to $\vec{q}$, and the azimuthal pion production angle ϕ_π.

deformation, and the interested reader will find many references in the introductions of earlier CEBAF proposals. [11, 12, 13]

Because the E2 and C2 amplitudes are small, when designing experiments to measure these amplitudes it is not sufficient to find observables which are sensitive to these amplitudes. One must also carefully examine these observables to see that the resulting errors will be small enough to make the measurement interesting. For the case of polarized beam and an unpolarized proton target, there are several cross section-like observables which are sensitive to the E2 and C2 amplitudes. However, these require either Rosenbluth separations (with attendant error amplification) or require apparatus with a great deal of out-of-plane acceptance in order to make believable separations of terms with $\cos\phi$ and $\cos 2\phi$ behaviour. [14, 15]. A precise asymmetry measurement of a sensitive observable would be very useful in the determination of E2 or C2. Such an observable exists in the case of C2.

The simplest measurement of a polarization observable which does not require a polarized target is that of A_e. This observable is the difference of the helicity dependent cross sections normalized to their sum. Figure 1 defines the kinematic variables often used in hadron electroproduction. Following Nozawa and Lee [15], we can write down the helicity dependent cross section in terms of electron LAB variables and pion CM variables as:

$$\frac{d^3\sigma_h}{d\Omega_e dE_e d\Omega_\pi} = \Gamma \frac{d\sigma_h}{d\Omega_\pi} = \Gamma[\frac{d\sigma^u}{d\Omega_\pi} + h\sqrt{2\epsilon(1-\epsilon)}\frac{d\sigma_e}{d\Omega_\pi}\sin\phi_\pi]$$

where

$d\sigma^u/d\Omega_\pi$ is the unpolarized cross section,

$d\sigma_e/d\Omega_\pi$ is the electron polarization cross section,

$$\Gamma = \frac{\alpha(\omega - Q^2/2M_p)}{2\pi^2 Q^2}\frac{E_{e'}}{E_e}\frac{1}{1-\epsilon}$$

and

$$1/\epsilon = 1 + \frac{2|\vec{q}|^2}{Q^2}\tan^2\theta_e/2.$$

where ω is the electron energy loss and $Q^2 = -q^2 = -(P_e\text{-}P_{e'})^2$ is the 4-momentum transfer. Then one can define the asymmetry,

$$A_e = \frac{1}{\sqrt{2\epsilon(1-\epsilon)}}\frac{(d\sigma^{h=+1}/d\Omega_\pi) - (d\sigma^{h=-1}/d\Omega_\pi)}{(d\sigma^{h=+1}/d\Omega_\pi) + (d\sigma^{h=-1}/d\Omega_\pi)} = \frac{d\sigma_e/d\Omega_\pi}{d\sigma^u/d\Omega_\pi}\sin\phi_\pi.$$

Note that A_e and $d\sigma_e/d\Omega_\pi$ both vanish in the electron scattering plane, where $\phi_\pi = 0$. Therefore out of plane acceptance is required in order to do the measurement. Also, because $d\sigma_e/d\Omega_\pi$ is much smaller than $d\sigma^u/d\Omega_\pi$, the resulting asymmetries are small.

In terms of interaction currents, A_e through the numerator is sensitive to $\mathrm{Im}(J_x J_z^*)$. Assuming the Δ decays into only s- and p-wave pions, then the multipole amplitudes one is sensitive to are in the combination $Im(S_{0+}M_{1+}^* + 6cos\theta_\pi S_{1+}M_{1+}^*)$, where the S_{1+} could have a resonant part. (One of the cross section-like measurements we decided to forego above is actually important and must eventually be carried out; the interference cross section, σ_I, will provide information about the *real* parts of products of multipoles with C2.)

At the heart of the model of Nozawa and Lee, which includes the effects of off-shell pion rescattering, lies the $\gamma N \rightarrow \Delta$ vertex function,

$$\Gamma_{\mu\nu} = G_M(q^2)K^M_{\mu\nu} + G_E(q^2)K^M_{\mu\nu} + G_C(q^2)K^M_{\mu\nu}$$

where $G_M(q^2)$ is the magnetic dipole (M1 or M_{1+}), $G_E(q^2)$ is the electric quadrupole (E2 or E_{1+}), and $G_C(q^2)$ is the charge form factor (C2 or S_{1+}). The $K_{\mu\nu}$ are kinematical tensors. In the rest of this proposal we will refer only to the G_C form factor, but the reader should keep in mind that the question being asked is whether there is a Δ component to the longitudinal current J_z or the S_{1+} multipole.

We want to emphasize that the extraction of the Δ contribution to G_C is somewhat model dependent. Not only does the Δ piece interfere coherently with the background caused by the Born diagrams, but the extracted multipoles are 'distorted' by pion rescattering. Thus

model dependencies and distortion effects will ultimately limit the precision with which G_C can be extracted.

One advantage of the reaction $e + p \rightarrow e + p + \pi^0$ over $e + p \rightarrow e + n + \pi^+$ is that pion electroproduction from non-Δ mechanisms is minimized. These non-Δ backgrounds, which interfere coherently with the Δ decay, will be called 'physics backgrounds'. It is well known that for W = 1232 MeV/c^2 a large fraction of the π^+ electroproduction cross section is due to the Born diagrams, while most of π^0 electroproduction is Δ mediated. In this manner we minimize model dependent errors due to theoretical treatment of the physics backgrounds. Some background is essential to us, of course, or A_e would vanish. If S_{1+} and M_{1+}^* were purely resonant, they would have the same phase and $Im(S_{1+}M_{1+}^*)$ would be identically zero. Inclusive $\vec{p}(\vec{e},e')$ measurements [11] such as $A_{LT'}$ are another means of making very precise measurements of sensitive polarization observables. The $A_{LT'}$ measurement proposed by Jourdan *et al.* is also sensitive to the $\mathrm{Im}(J_x J_z^*)$, but the inclusive reaction contains contributions from both charged and neutral pion production channels. A comparison of the two measurements will be very interesting.

We are proposing a precision measurement of A_e at $Q^2 = .3$ and $.4$ (GeV/c)^2 for invariant Δ masses of 1182, 1232, and 1252 MeV/c^2. Using the out-of-plane acceptance of the SOS-HMS system, we will simultaneously cover $\theta_\pi^{CM} \simeq$ 150-180 degrees. This will be an exclusive measurement of neutral pion electroproduction. Calculations [16, 15, 24] predict large variations in A_e as a function of Q^2, W, and θ_π^{CM}.

It is expected that careful measurements at CEBAF and other laboratories on a number of observables will be required in order to fully test models such as that of Nozawa and Lee, or that of Laget. Only when the model dependences are fully understood will we know what error to assign to the extracted value of G_C.

1.2 Theoretical Support

There is a great deal of interest among the theory community on the possibility of deformation in the nucleon and Δ. This interest has taken many forms. Raskin and Donnelly [17] have written down expressions for various polarization observables in the 1-photon exchange approximation for decay of a spin-3/2 hadron to a spin-1/2 hadron + pion. Although their formalism does not account for the Born backgrounds or pion rescattering, their formulas nevertheless reveal the kinematic dependences of various observables, and they relate these observables directly to multipole amplitudes. This work gives valuable insight to the experimentalist in the design of experiments.

The RPI group has struggled to extract the E2/M1 ratio from existing data, taking care in their models to separate Δ from non-Δ transition amplitudes. [7, 8] The extracted values of E2/M1 vary by more than what the model dependence is claimed to be, but all agree that the magnitude of the ratio is small, <5%. While the group continues to investigate these model dependences, [9, 10] it is their opinion that better quality data than those found in the existing data base would be very helpful.

Nozawa and Lee [14, 15] use a model hamiltonian which was constructed so as to be both unitary and gauge invariant. They found the effects of πN off-shell rescattering following

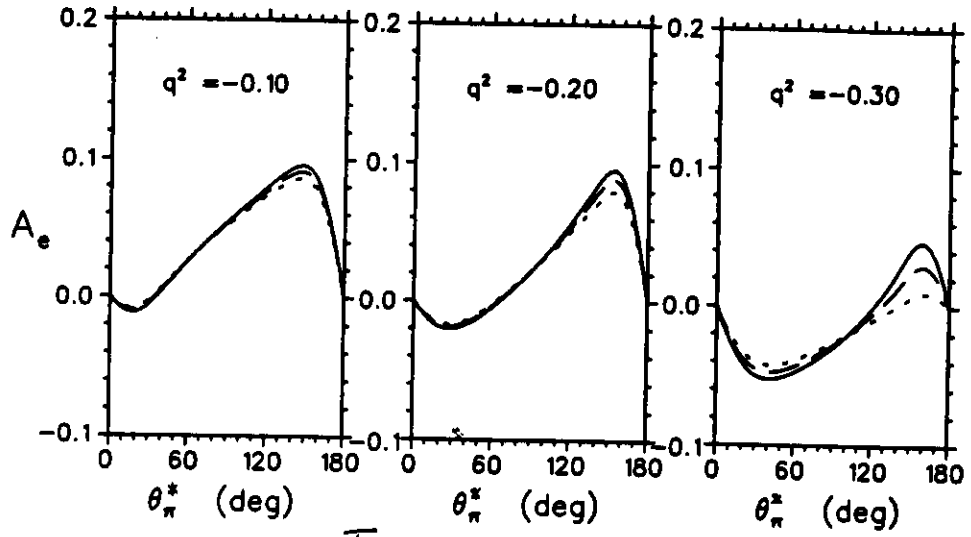

The asymmetry A_e. In the calculation $\epsilon = 0.9$ is used.

Figure 2: Predicted dependence of A_e on Q^2 and θ_π. Calculations are from Nozawa and Lee.

Born production affected the cross sections by as much as 50%. Most existing models which impose unitarity by Watson's theorem do not find such large effects.

Partly in response to existing experimental proposals, calculations have been done [14, 15, 16] which demonstrate the sensitivity of various observables to the G_C and G_E transition amplitudes. In particular, A_e (or Σ_e in Laget's nomenclature) has been found to be sensitive to the value of G_C. Both calculations agree about the systematic behaviour of A_e: the asymmetries are fairly small (5-10%) and decrease rapidly between .1 and .3 $(GeV/c)^2$ but with increasing sensitivity to the value of G_C. (See Figure 2.)

Laget has found that the overall normalization of cross sections calculated for $p(e, e'\pi^0)p$ was sensitive to the value of $G_M(q^2)$ used. This particular normalization problem disappears when a ratio of cross sections such as A_e is calculated. Then one is sensitive only to the ratio $G_C(q^2)/G_M(q^2)$, which is often assumed to be 1. Real photon measurements would be another way of avoiding this model dependence, but then one would be limited to E2 sensitive measurements.

1.3 Related Proposals

Due to the importance of determining the G_C and G_E form factors in the N→ Δ transition, it is not surprising that many such experiments have been proposed or are in progress. The reader is referred to Appendix A for a list of all experiments that are known to us.

Here we will only discuss the various measurements of A_e. As mentioned above, a measurement of A_e is perhaps the simplest such experiment involving polarization, provided one has the capability of measuring Δ decay products above or below the electron scattering plane. However, systematic errors still must be controlled and the small size of the asymmetries demands high statistics. There are presently two other proposed measurements of A_e: one at CEBAF by Burkert[13] and one at Bates by Papanicolas[18]. These two proposals and the present one are very distinct, with no overlap in Q^2. Many of the systematic errors are completely different due to the range of apparatus employed. Also, some of the reactions measured are even different, although all three measure $e + p \rightarrow e' + \pi^0 + p$.

The Bates measurements will be made at low Q^2 where the predicted sensitivity to G_C is small. The overall magnitude of A_e is relatively large, however, so counting statistical errors are not a problem. Absolute knowledge of scattering angles is made difficult by the fact that an out-of-plane (OOP) spectrometer system is employed. Test measurements were made before the recent Bates shutdown, and the group is working to understand and control systematic errors[19].

Due to the large acceptance of the CLAS, the Burkert *et al.* measurements will cover a large range of Q^2 and θ_π simultaneously. These measurements will provide an invaluable survey of pion electroproduction at relatively high Q^2 in a reasonable time if the goal of 10^{34} luminosity can be achieved. However, for the range of out-of-plane angles which are accessible to the HMS-SOS system, the large acceptance of the CLAS is compensated by the 4 orders of magnitude greater luminosity of the SOS-HMS system in Hall C. This is particularly important at low Q^2 (a region not covered in the CLAS survey) where A_e is predicted to vary rapidly on the scale of only .1 $(GeV/c)^2$, or *half* the proposed CLAS binning in Q^2.

2 The Experiment

2.1 Overview

There are several considerations which make a useful A_e measurement possible in Hall C:

- Calculations show that the sensitivity of A_e to the G_C transition form factor is largest near θ_π^{CM} = 20-30 degrees and 140-170 degrees.
- Out-of-plane angles as large as 6 degrees are possible with good acceptance in the combined HMS-SOS system. In particular, the HMS has a vertical acceptance of ± 4.3 degrees.
- For $Q^2 \geq .3$, we are able to access most of the interesting region of θ_π^{CM} = 140-170 degrees provided we detect the proton. Acceptance of θ_π^{CM} increases with Q^2 until 3.7 $(GeV/c)^2$, when all pion CM angles become accessible.

In addition, over the proposed range of Q^2 we are usually able to take advantage of the special kinematics of the reaction $e + p \rightarrow e' + \Delta$ (see Fig. 3). For a given beam energy and

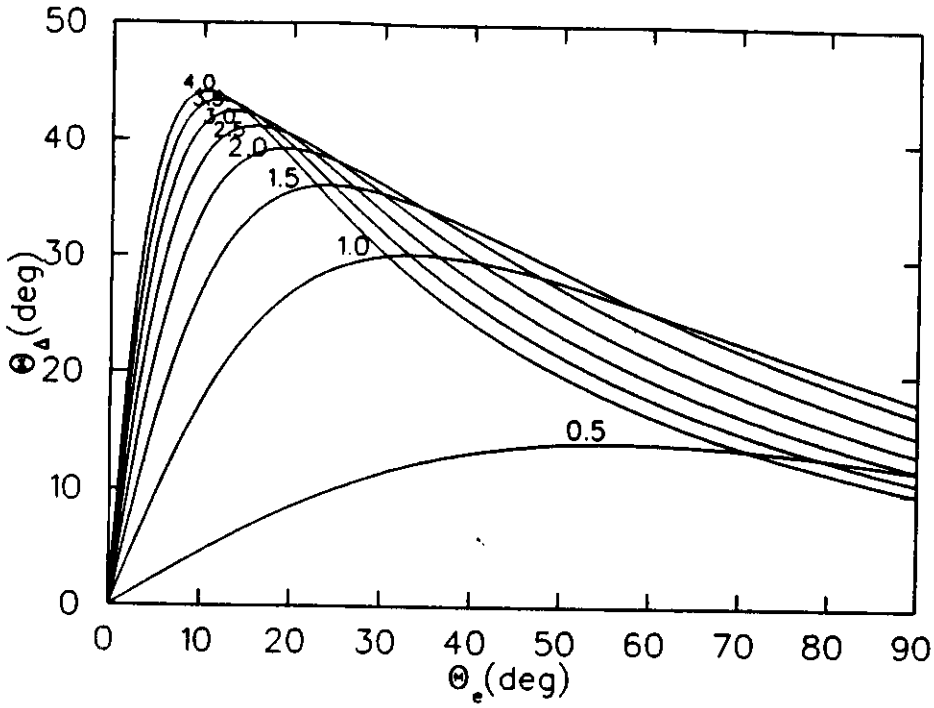

Figure 3: θ_Δ versus θ_e for several beam energies.

Table 1: Expected performance of the HMS and SOS (pt-to-pt tunes in x,y).

	dp/p	dθ mrad	dϕ mrad	$\Delta\Omega$ msr
HMS	10^{-3}	2	2	7
SOS	10^{-3}	2	2	7.5

W, an electron angle exists such that first, the error in predicting the Δ angle becomes very small, and second, the Jacobian for the transformation from the CM frame to the lab frame becomes very large.

For the proposed range of Q^2, electrons will be detected in the HMS and protons in the SOS. Spectrometer magnet tunes which are point-to-point in y will be used in order to maximize the angular acceptances. The resulting momentum resolutions for the two spectrometers will conservatively be 10^{-3}. Table 1 contains the expected performance of each spectrometer in this experiment.

The configuration of the HMS detector package will be the standard one found in the CDR on page 54 (Fig. 4a). Two wire chambers will be followed by an x-y plastic scintillator hodoscope, a gas Cerenkov detector, another x-y hodoscope, and finally a Pb-glass shower counter. As this will be the electron arm, the HMS hardware trigger will be

(S1XOR•S1YOR)•(S2XOR•S2YOR)•Cerenkov. For the SOS detector we will require one element which is not included in the standard package found in the CDR on page 121 (Fig. 4b). In order to avoid unnecessary triggers due to pions, we will reject pions in hardware using a Cerenkov detector. The SOS trigger will be (S1XOR•S1YOR)•(S2XOR•S2YOR)•(No Cerenkov). While the event of interest will be HMS•SOS, prescaled HMS and SOS singles events will also be acquired as a check of the detector systems.

The Hall C low power (ie, 50W-100W) liquid Hydrogen target will be used. The target design and construction are being led by Jim Pace, Hall C cryogenics engineer. This target as presently planned will be a cylindrical vessel 15 cm long with etched Aluminum endwindows. Consultations with John Mark of SLAC and the procurement of target components are in progress.

The polarized electron source to be used in experiments at CEBAF is under development by a group led by Larry Cardman of NPL at the University of Illinois.[20] The source is expected to be able to deliver up to 200 microamperes of electrons with a polarization of .49. It will be possible to flip the helicity of the beam via a Pockels cell at rates approaching 1 KHz. Stability of the current and polarization under helicity flips are expected to be better than 10^{-5}. Spin orientation apparatus is under construction at the University of Illinois. Drifts in the polarization are likely to be dominated by the stability of the spin precession in the accelerator. The fact that Accelerator Division has purchased 10 ppm ($1{\cdot}10^{-5}$) current regulated power supplies for the magnets is very encouraging. A back of the envelope estimate which neglects magnetic field gradients over dimensions of the CEBAF beam suggests that the precession angle will be unstable at 4 GeV to $\pm.072$ degrees. Short term stability (minutes) of the current is that of the laser intensity, or 10^{-2}. At high currents the cathodes age rapidly and the 1/e lifetimes are about 24 hours. A double source will be used so that polarized beam production can continue during refurbishment of the aged cathode. We estimate polarized source down time as 1 hour in 24 hours.

The beam polarization will be monitored with a Moeller polarimeter. If necessary, Hall C will assume responsibility for the construction of the polarimeter. However, users in the A_{LT} and G_E^0 collaborations are also considering taking on this responsibility. We assume conservatively for the error estimates below that we will be able to determine the absolute polarization of the beam to within $\pm 5\%$.

Miscellaneous beamline hardware which will be required for the experiment includes a beam rastering system to prevent LH_2 target destruction, beam position monitors (BPM's), and an ion chamber downstream of the target to monitor the beam current. This equipment will also be required by the majority of Hall C experiments. The BPM's will be purchased from Accelerator Division and interfaced to the Hall C controls HP. The beam raster and ion chamber will be built by Hall C personnel, and the run permit will be interlocked to satisfactory raster operation (among many other things).

Finally, we note that because we continuously measure $\theta_\pi^{CM} = 180$ degrees (where A_ϵ must vanish), we have a limited check that false asymmetries are not being introduced by hardware or software.

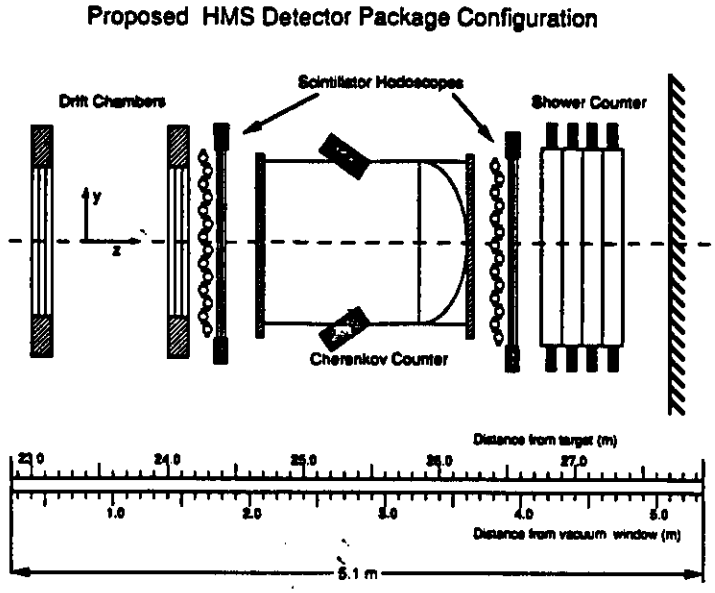

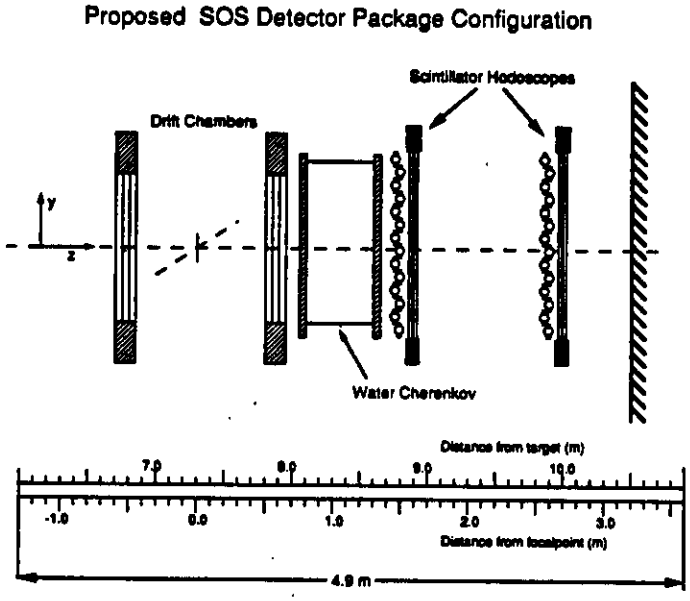

Figure 4: Schematic diagram of the HMS and SOS detector packages required for this experiment.

Table 2: Kinematics for e+p→Δ(1232).

Q^2	P_{beam} (MeV/c)	HMS $\theta_{e'}$ (deg)	HMS W (MeV)	$P_{e'}$ (MeV/c)	$P_{e'}/P_{beam}$	θ_Δ (deg)	P_Δ (MeV/c)	ϵ
.302	2300	15.25	1182	1864.	.81	44.3	702.	
.298	1750	21.25	1232	1252.	.70	37.9	739.	.89
.298	1540	25.75	1282	975.	.63	32.6	786.	
.398	3150	12.5	1182	2663.	.85	46.3	797.	
.402	3200	12.5	1232	2647.	.83	42.9	842.	.96
.400	2300	18.5	1282	1681.	.73	37.1	885.	

2.2 Kinematics

In this experiment the centroid of the invariant mass W will be fixed at particular value while the squared 4-momentum transfer, Q^2, is varied. Normally one would be free to choose the beam energy, but here that is not the case. For a given beam energy Pe and invariant mass W, there is a 'magic' angle at which the derivative $d\theta_\Delta/d\theta_{e'}$ vanishes (see Fig. 5). (The magic angle is simply the largest laboratory angle for the virtual photon.) The variation with W is sufficiently slow to allow us to measure a large fraction of the Δ resonance in one kinematic setting. In these kinematics not only does the error in the prediction of θ_Δ vanish to lowest order, but the Jacobian $d\Omega^{CM}/d\Omega^{LAB}$ has a spike. Because of these advantages we have selected these 'magic' angle kinematics for most of our settings. However, for fixed invariant mass W there is a 1-to-1 correspondence between Q^2 and the beam energy, which leaves us no freedom to choose the beam energy. Table 2 gives the kinematics for the $e + p \rightarrow e' + \Delta$ system.

For Q^2 = constant it is not possible to acquire the entire Δ resonance at a single setting of the beam energy, HMS angle, and SOS angle. (See Fig. 5.) For fixed beam energy and electron arm angle, the θ_Δ angles for invariant Δ masses of 1232±50 MeV are somewhat outside the SOS angular acceptance for W = 1232. However it is not sufficient to simply change the SOS angle since the kinematics are then no longer magic. In order to keep Q^2 fixed while retaining magic kinematics as W is varied, the beam energy and *both* spectrometer angles must be changed.

Table 3 has the kinematics for the proton due to Δ decay. The fourth column gives the range of θ_π^{CM} angles that will be covered in this experiment. The A_e predictions in Figure 2 suggests that this region is particularly sensitive to G_C for Q^2 = .3 and .4 $(GeV/c)^2$. Plots of proton kinematics with respect to the virtual photon direction are found in the Appendix B.

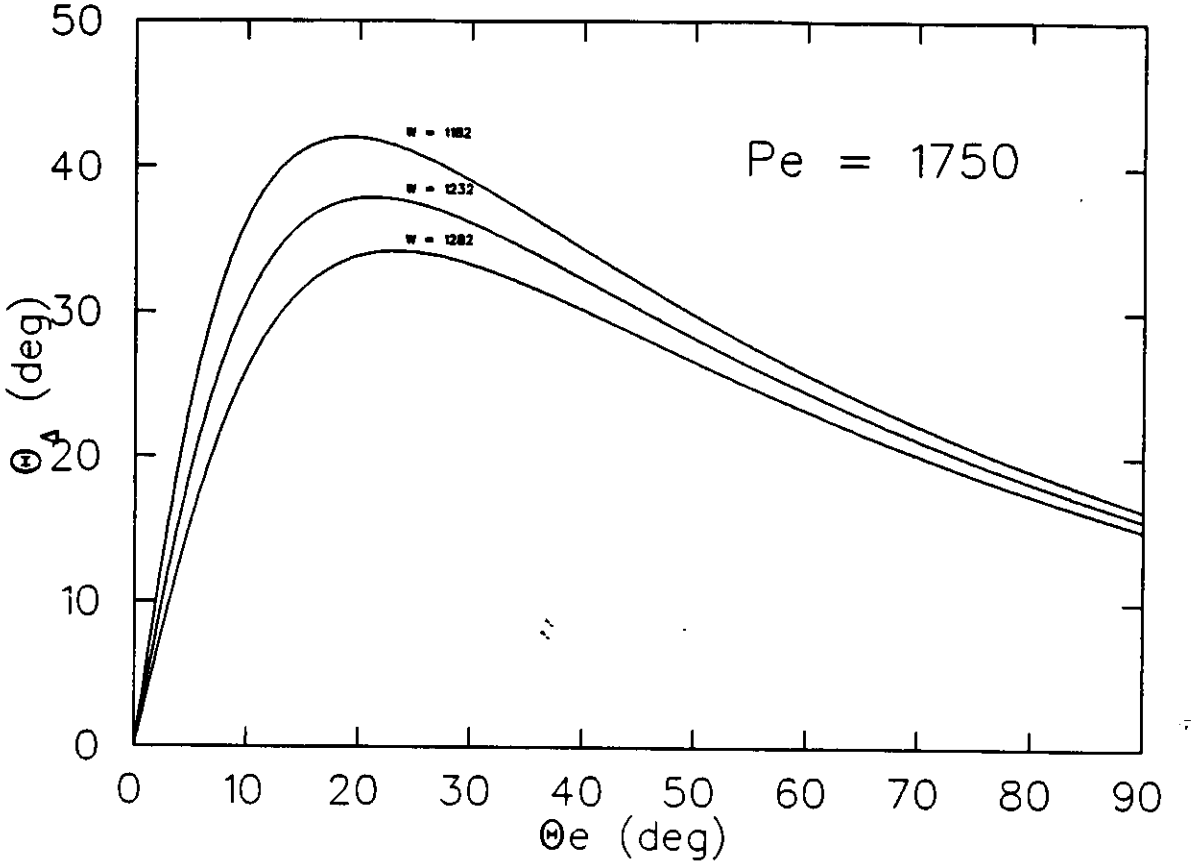

Figure 5: θ_Δ versus θ_e for P_{beam} = 1750 MeV/c and several values of the invariant Δ mass.

Table 3: Kinematics for $\Delta(1232) \rightarrow p + \pi^0$.

θ_p wrt $\vec{q}$ (deg)	Nominal Q^2 e+p→ e + Δ	W (MeV)	P_p^{SOS} (MeV/c)	θ_π^{CM} wrt $\vec{q}$ (deg)	Missing Mass Resolution (MeV/c²)
0-6	.3	1182	779.-762.	180.-154.0	
		1232	847.-831.	180.-157.8	3.8
		1282	920.-905.	180.-159.8	
	.4	1182	864.-841.	180.-151.	7.4
		1232	938.-917.	180.-155.3	
		1282	1007.-987.	180.-157.8	

Table 4: Time of flight over 1.m for p's and π's for P_{min} and P_{max}.

P (MeV/c)	β_p	TOF_P (nsec)	β_π	TOF_π (nsec)	ΔTOF_{min} (nsec)
760.	.630	5.29	.983	3.39	1.90
1000.	.729	4.57	.990	3.37	1.20

2.3 Particle Identification

Electrons in the HMS will be distinguished from pions with inefficiencies of at most 10^{-3} by a signal in the UVA Cerenkov counter[22]. The working gas will be CO_2 at less than .5 atmospheres, providing a Cerenkov threshold for pions of 6.6 GeV/c. The Cerenkov will be placed before the first scintillator hodoscope in order to minimize pion rejection inefficiencies due to knock-on electrons. At the HMS angles and momentum settings for the proposal, the π^-/e^- ratios range from 10^{-2} to 1. Therefore, the Cerenkov detector alone will be sufficient to reject essentially all pions. Lead glass shower counters will provide redundant pion rejection offline with inefficiencies of 10^{-2}-10^{-3}. For HMS momentum settings below about 900 MeV, pions and electrons will be separated by > 1 ns in TOF. This TOF particle identification capability could be used as another check of our pion rejection inefficiencies.

Pions and positrons in the SOS will be rejected in hardware by the presence of a signal in an H_2O Cerenkov counter. We will use the same counter discussed in J. Napolitano's proposal to PAC5 (a measurement of p(γ,k)Λ and p(γ,k)Σ at 90 degrees CM). Although not in the CDR, this Cerenkov would be generally useful and can be built by Hall C or one of the collaborating institutions using construction funds. The protons of interest in this experiment are rather slow (β = .57-.73), but will nevertheless radiate in a medium with n $\geq = 1/\beta = 1.37$ such as lucite (n = 1.49). Water however has an index of refraction of only 1.33, which corresponds to a Cerenkov β threshold of .752 . Kaons, Pions, and electrons will radiate at all the momentum settings planned for this experiment.

The advantage of using a Cerenkov detector over a TOF measurement is that in this manner we do not have to chop the beam. This allows us to minimize random concidences for a given beam current. Nevertheless, redundant π-p discrimination will be available offline in the form of TOF between the SOS S1 and S2 hodoscopes. Together with prescaled SOS singles without the Cerenkov in the coincidence, this will also provide an independent means of verifying the rejection efficiency of the H_2O Cerenkov. The separation between the hodoscopes will be only 1-1.5m, because we will place the Cerenkov detector just behind the second wire chamber in order to avoid knock-on electrons. See Table 4 for the π-p TOF separations for d = 1m at P_{min} and P_{max}.

The ratio of π^+/p in the SOS is expected to be of order 1 for all settings [23] so heroic measures are not required to reject pions. The Cerenkov should be able to reject pions with inefficiencies of order 10^{-3}.

It will be possible to distinguish protons and deuterons both by TOF and pulse height in the scintillator hodoscopes. TOF with respect to the RF will also be available, using the

HMS to tag the originating beam burst. In that case the flight path through the SOS is about 10m. A consistency check will be performed to ensure that the scattered electron and proton came from the same beam burst. For this reason we use a resolving time of 2 ns (ie, 1/500MHz) when calculating our off-line reals/randoms ratios.

Tables of the total target related rates, trigger rates, and particle ratios for the HMS and SOS are found in Appendix C. The total rates are reasonable and the on-line reals/random ratios using a resolving time of 10 ns are of order 1.

2.4 Non-physics backgrounds

Once a combination of on-line hardware and off-line software have determined that there was a coincidence between an electron in the HMS and a proton in the SOS arising from the same beam burst, there remain several possible backgrounds of the more usual incoherent 'non-physics' variety: radiative tails, backgrounds from A(e,e' p)X in the target endcaps, and other resonance decays which lead to final state protons.

Quasi-free knockout from the target endcaps will not be accepted by the SOS in this experiment. With a point-to-point magnet tune in Y the length of target accepted is $\pm 2.5\text{cm}/\sin(\theta_{SOS})$. At the smallest SOS angle planned, 26.3 degrees, the accepted target length will then be 11.3cm. Thus if a 15cm LH_2 vessel is used, there should be no background from the endcaps except for a small tail due to finite resolution effects. If commissioning studies show that Murphy's law prevails, then we will design tungsten slits to screen the endcaps during the experiment. Somewhat redundant reconstruction of the z coordinate will be also made on the HMS side.

Backgrounds from radiative tails with large energy loss will be removed by a cut on the mass of the π^0 which will be reconstructed from the electron and proton 4-momenta. This same cut will be used to remove backgrounds from other reactions which are not of interest. Assuming conservatively that the momentum resolutions in both spectrometers are 10^{-3}, and the in-plane scattering angle resolutions in both spectrometers are 2.0 milliradians, and vertex resolution in the y coordinate is $\pm$ .6cm, then the missing mass resolution in this experiment will be $\leq \pm$ 10 MeV/c^2, with an average missing mass resolution of about $\pm$ 5 MeV/c^2. This is certainly sufficient to exclude 2π production and the relatively small amount of Compton scattering. There may be some interesting physics in the Compton scattering which will end up on tape. However, at the rates we envision the reals/randoms ratios will be of order 1 after all off-line cuts, and together with the 2 orders of magnitude lower statistics, any small A_e value would be impossible to measure.

2.5 Out of plane acceptance

In Appendix C we discuss angular acceptances for the HMS-SOS spectrometer system. Preliminary results have been obtained using simulation which assumes that the virtual photon directions lie on a locus which slices vertically through the SOS angular acceptance. For fixed W, the invariant mass of the Δ, this is an excellent approximation. For a fixed proton decay cone angle, events were generated all along the vertical locus. The fraction of events

which intersect the SOS aperture then gives an unnormalized acceptance for this particular out of plane angle, θ_p. When this procedure is repeated for all accepted θ_p (roughly 0 to 6 degrees, in .5 degree bins), the acceptance can be normalized. Thus if N real coincidence events are written to tape, the fraction of events at θ_p = 4 degrees (for example) can be determined.

As one might expect, given the limitations of the SOS vertical acceptance, the probability of detecting a proton at $\theta_p = 6$ degrees is significantly smaller than the probability of detecting a proton at .5 degrees. It is shown in Tables 7 and 8 of Appendix E that only about 7% as many events will be detected at 6 degrees as at .5 degrees. (The acceptance is fortunately a slow function of W.) A high statistics measurement of A_e at $\theta_p = 6$ degrees would lead to unreasonably long counting times, but at 4 degrees the relative acceptance is a hefty 45% and the physics are still interesting.

A detailed study of Q^2, W, and θ_π acceptances will be made with a new version of Paul Ulmer's code MCEEP.[21]

2.6 Error Estimate

Our goal in this experiment is to determine A_e at each kinematic setting to better than 7.5%. In Appendix E we examine the effects of statistics, uncertainties in the beam polarization, Q^2 resolution, and absolute uncertainty in Q^2. We conclude that this goal is a reasonable one. In Figure 6 we show a plot of A_e for Q^2 = .4 $(GeV/c)^2$ from Nozawa and Lee [24]. In the region of 160 degrees CM, the curves from top to bottom represent G_C values of .15, 0, and -.15. We have plotted an estimated error bar on Figure 6 [24] for an angle corresponding to 4 degrees (LAB) and A_e = .03 . The bin is 2 degrees wide in CM angle. The sensitivity of the experiment is obviously high. If the calculations were perfect we would be able to determine G_C to the level of about $\pm$.01. Such faith is unrealistic, but these measurements will severely test models such as that of Nozawa and Lee, and we should be able to extract a value for G_C and assign an error once the model dependences are understood.

2.7 Beam Request

Our data rates are based on the following constraints:

1. The beam current should not exceed 50μamps. In a 15 cm LH_2 target this corresponds to at least 42W of refrigeration power required. The design goal of the Hall C low power target is 50W-100W.

2. The ratio of real coincidences to random coincidences should be of order 1, assuming an on-line coincidence timing window of 10 ns.

3. The total coincidence trigger rate should not greatly exceed 1KHz. Since the fastbus TDC's require about .25 msec to digitize, the deadtime will rapidly increase above 1KHz. Furthermore, for our expected event lengths, the writing capacity of a single VCR drive will be exceeded.

The laboratory triple differential cross section for protons can be derived from the pion CM version from section 1.1 as

$$\frac{d^3\sigma}{d\Omega_e dE_e d\Omega_p} = \Gamma \frac{d\sigma}{d\Omega_p^{CM}} \frac{d\Omega_p^{CM}}{d\Omega_p^{LAB}}.$$

where all the quantities on the left are now in the LAB and and using the fact that $d\sigma/d\Omega_p^{CM} = d\sigma/d\Omega_\pi^{CM}(\pi - \theta_p)$. For the proton center of momentum differential cross section, 7.5 μbarns/sr is a reasonable average for the cross section averaged over the Δ resonance for θ_π between 150 and 180 degrees. [25]

The coincidence rate in Hertz is then:

$$R = C \frac{d^3\sigma}{d\Omega_e dE_e d\Omega_p} \Delta P_{HMS} \Delta\Omega_{HMS} \Delta\Omega_{SOS} Amperes Nuclei$$

where the constant $C = (6.25{\cdot}10^{18}$ electrons/C$)(1{\cdot}10^{-30}$ cm$^2/\mu$barn) and $Nuclei = 7{\cdot}10^{22}$ nuclei/cm^2 for a 10 cm LH2 target.

Note that in our use of the cross section formula above we have averaged over solid angles which are large relative to the scale of laboratory angles we are interested in. Likewise, we have averaged over momentum bites which are large relative to the the scale of energies which will cause significant variations in W, the invariant mass. In other words, we now have an average count rate estimate which tells us nothing about the rate at extreme out of plane angles, or what range of W we have sampled. For that we need the acceptance studies found in Appendix C.

In Appendix E we show that in order to achieve errors of 7.5%, we require $1.5{\cdot}10^6$ counts per angle bin. Each bin in CM angle is 2 degrees wide. The coverage in θ_π^{CM} is somewhat different for the different kinematic settings (generally increasing with Q^2); the anticipated number of bins for each is found in Table 5. In Appendix C we show that due to the decreasing acceptance for larger out of plane angles, along with the fact that each acquired event must be weighted by the factor $\sin(\phi)$, the naive estimate of $1.5{\cdot}10^6$ counts per angle bin must be increased by a factor of 1/(fudge factor)= 2. Furthermore, because we will bin our data in 10 MeV bins, we must extend our counting rate by an additional factor of 4. (Each SOS bite has an acceptance of about 80 MeV, but the fact that we take three bites for different but overlapping W reduces the extra time needed to only a factor of 4.)

Thus we require 2x4x1.5$\cdot10^6 = 1.2{\cdot}10^7$ events per angle bin on average. (The raw data will fill a few hundred 5GByte tapes.) Table 5 contains the time estimate for each configuration. After including overhead for kinematic setting changes (3 hours each), retuning of the beam energy (24 hours for each retune), Moeller polarimeter runs (we assume 1 hour per 12 hours of production), and polarized source servicing (1 hour per 24 hours of production), the total beam request is 787 hours.

The final statistical errors on each angle bin will be presented to the PAC in November after acceptance studies with MCEEP are complete.

Table 5: Count rate estimate for 7.5% total errors.

Setting	Bins	Total Events $1.2{\cdot}10^7$*Bins	Beam Current μamps	Real Coinc. Rate	Time (hours)
1	13	$1.56{\cdot}10^8$	25	604	72
2	11	$1.32{\cdot}10^8$	50	432	85
3	10	$1.2{\cdot}10^8$	50	229	146
4	15	$1.8{\cdot}10^8$	15	797	63
5	13	$1.56{\cdot}10^8$	20	309	140
6	11	$1.32{\cdot}10^8$	15	738	50
subtotal					556
w/overhead					787

3 Manpower

This experiment will be lead by CEBAF personnel and assisted by collaborators who are interested in the physics and who are currently developing hardware for the Hall C program. It is assumed that graduate students and postdocs from collaborating institutions, particularly those stationed in Hampton Roads, may wish to participate in the experiment. ODU, for example, would like to send one graduate student for the run. We are looking into the possibility of collaborating with the University of Illinois and the University of Virginia, whose interest and experience in these measurements would be invaluable.

The spokesperson will assign a student to the experiment who will use this as his/her doctoral thesis. This student will participate in the simulation, error analysis, detailed run plan, and data analysis of the experiment. The student will also be heavily involved in the development of detectors for this and other experiments in the Hall C program.

4 Summary

All the hardware required for the proposed experiment is expected to be available in the endstation at startup in 1994. Furthermore, the requirements on momentum resolution and angular resolution are very modest, as the requirement on absolute determination of the scattering angles. The detector packages we require are standard equipment except for the water Cerenkov, and that should be relatively simple and inexpensive to manufacture. The particle identification capabilities of the detector packages as we have described them are several orders of magnitude better than what is necessary. Stability of the beam mean energy at the level of 10^{-3} is sufficient for the experiment. The cross section of $p(e,e'p)\pi^0$ is relatively large, and the reals to randoms ratio online is of order 1. Offline cuts will increase the reals to randoms ratio by 10^2.

In short, a precise and important coincidence measurement can be made in endstation C

shortly after startup, provided that a beam polarization of at least 50% at a current of 50 microamperes is available, and that the requested beam energies can be delivered. Finally, we would like to point out that the six energies required for this experiment may be difficult to schedule in a continuous run unless the experiment takes place before the Hall A start of physics.

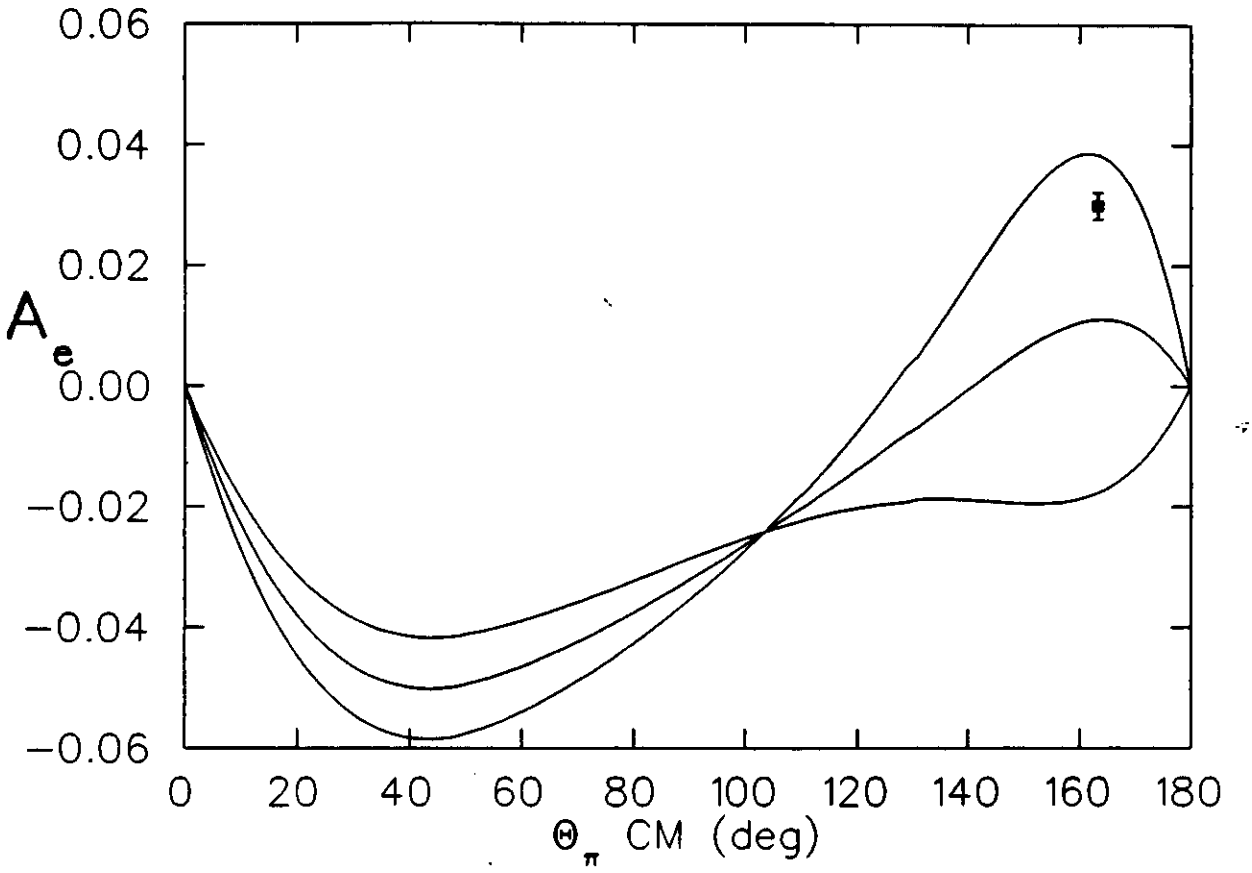

Figure 6: Predicted A_e versus θ_π for $Q^2 = .4$ and $W = 1232 \pm 5$ MeV/c^2. Calculations are from Nozawa. A representative error bar is shown for an angle where the relative acceptance is about 45%.

A Measurements proposed or in progress

Table 6: Other proposals to measure G_C and G_E form factors in N→Δ(1232) transition.

Lab	Spokesperson(s)	Reaction/ Observable	Q^2	Stated Physics Focus
CEBAF	Jourdan	$\vec{p}(\vec{e},e')$ A_{LT}	.2-1.4	G_C
Bates	Papanicolas	$p(\vec{e},e'p\gamma)$ $e+p\rightarrow e+p+\pi^0$ $e+p\rightarrow e+p+\gamma$ A_e, ϕ dependence of $d\sigma/d\Omega$	.07-.12	E2/M1 C2/M1
Bates	Lourie, Burkert	$p(\vec{e},e'\vec{p})\pi^0$ Most in-plane structure functions.	.12	S_{1+}, M_{1+}, E_{1+}
CEBAF	Burkert, Minehart	$p(\vec{e},e'p)\pi^0$ $p(\vec{e},e'\pi^+)n$ $d(e,e'\pi^-)pp_s$ ϕ dependence of $d\sigma/d\Omega$	.2-4.	S_{1+}, M_{1+}, E_{1+}
CEBAF	Burkert, Minehart	$p(\vec{e},e'p)\pi^0$ $p(\vec{e},e'\pi^+)n$ A_e	.5-2.	$Im(S_0 M_{1+}^*)$ $Im(S_{1+} M_{1+}^*)$
LEGS	Sandorfi	$p(\vec{\gamma},\pi^0 p)$? Σ?	0.0	E2/M1
CEBAF	Mack	$p(\vec{e},e'p)\pi^0$ A_e	.3-.4	G_C

B Kinematics of tagged Δ decay

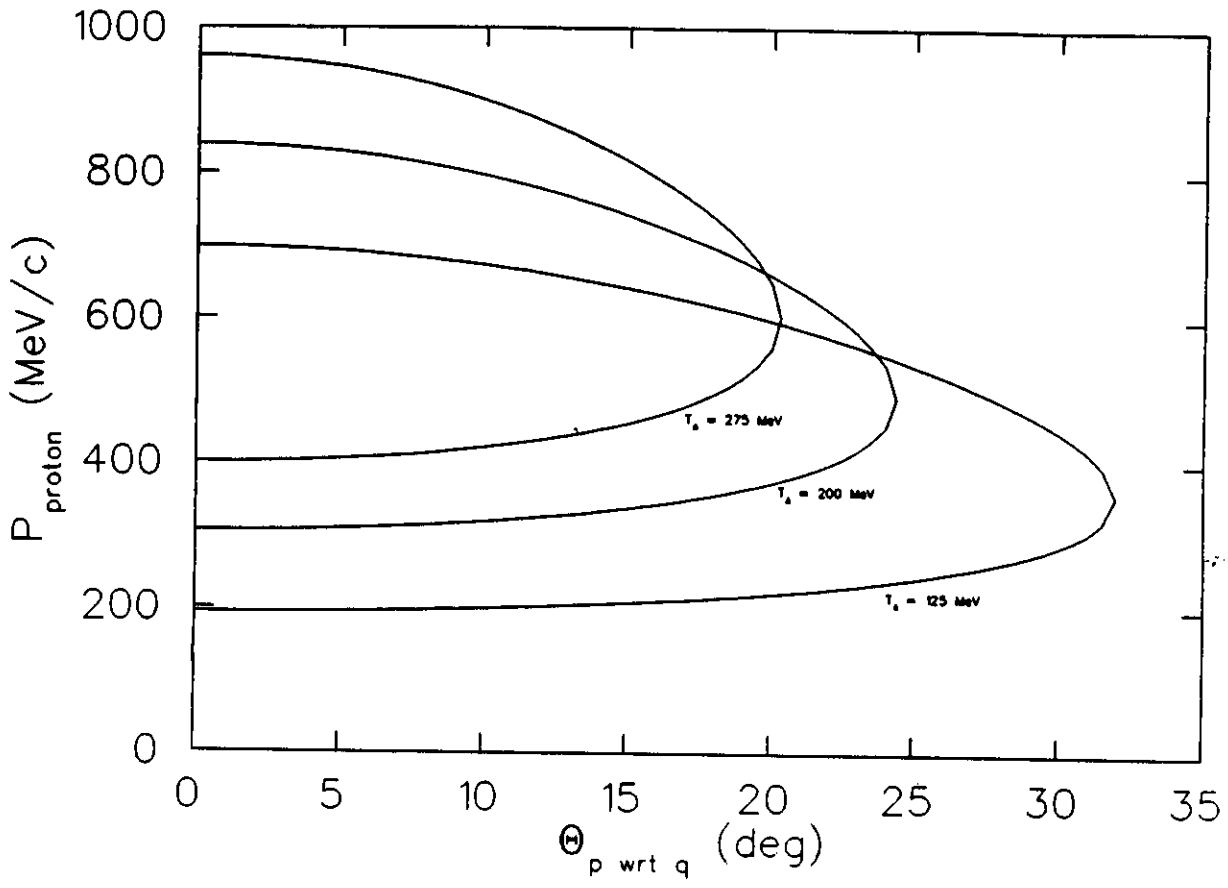

Figure 7: P_p versus θ_p for several kinetic energies of the Δ. (W = 1232) The angle θ_p is measured with respect to $\vec{q}$. For each locus, the highest proton momentum corresponds to $\theta_p^{cm} = 180$ degrees ($\theta_\pi^{cm} = 0$ degrees.) This experiment will measure θ_p as large as 6 degrees.

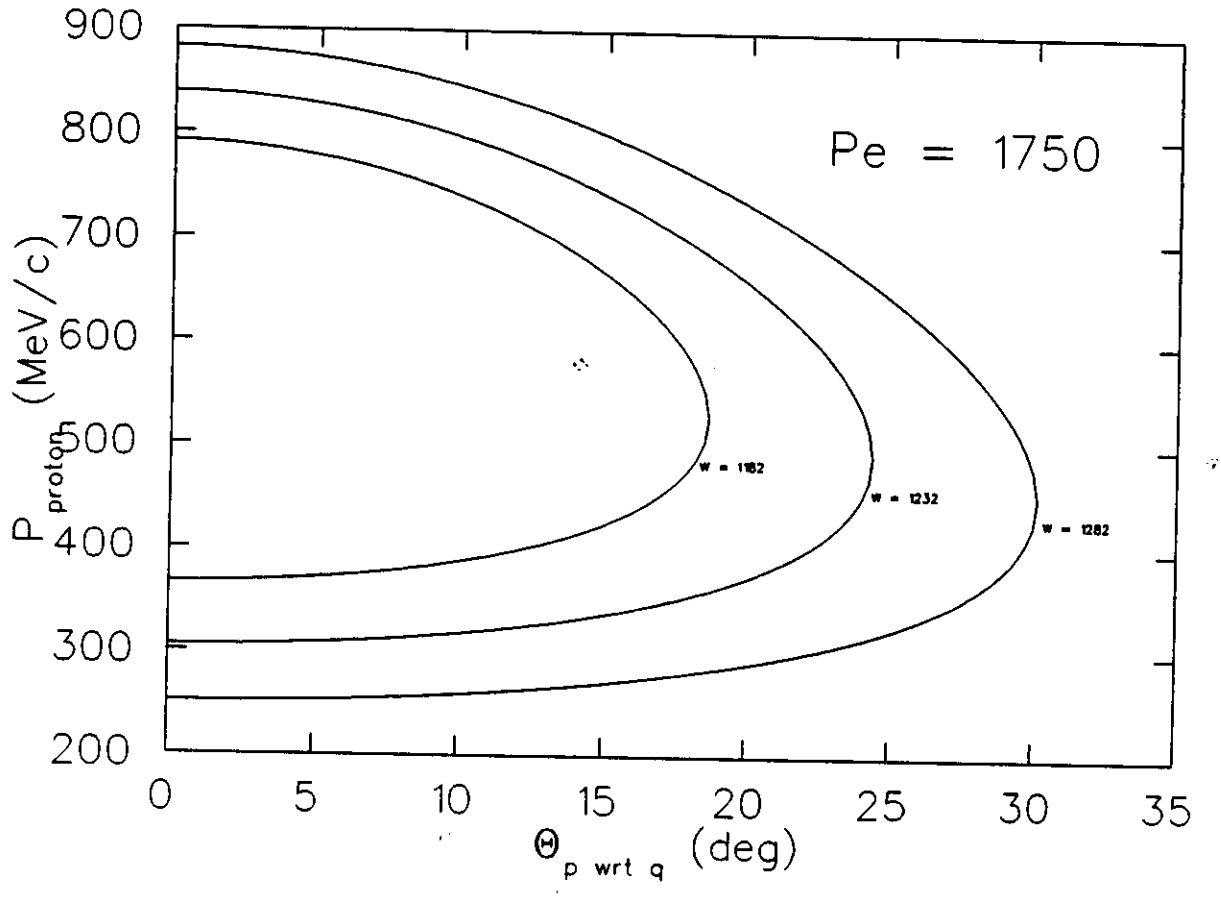

Figure 8: P_p versus θ_p for several values of the Δ invariant mass. The tagged Δ kinetic energy is 200 MeV.

C Spectrometer Angular Acceptances

In this section we discuss the somewhat complicated out of plane angular acceptance of the HMS-SOS system. We begin with Figure 9, which shows schematically a view looking upstream with the HMS and SOS on opposite sides of the beam. If an electron is detected near the top part of the HMS vertical acceptance, and the SOS is in the proper position, then we may detect protons at a laboratory angles of somewhat more than 6 degrees. This is not a very large laboratory angle, but for neutral pion photoproduction it allows us to cover an interesting region of θ_π^{CM}.

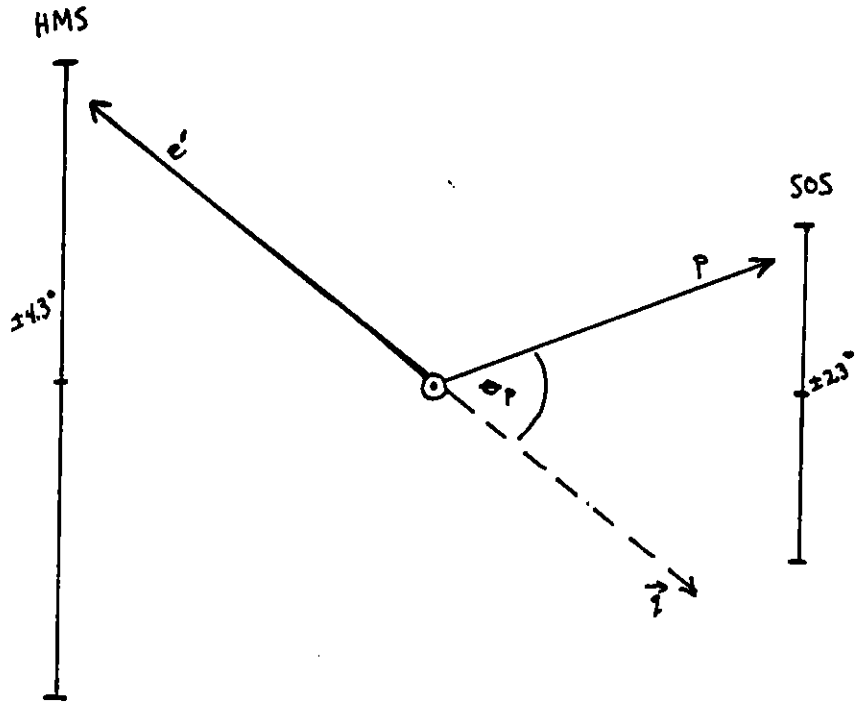

Figure 9: Schematic diagram showing how out of plane acceptance arises in a dual spectrometer system.

Next we want to look along the virtual photon direction as in Figure 10. We again assume that the HMS has detected an electron near the edge of its vertical acceptance, 4 degrees out of plane. The circles correspond to the intersection of proton decay cones with the SOS aperture. Each circle corresponds to a given center of mass angle for the decay. From the figure we can see that for such extreme rays there is no possibility of detecting protons at θ_p much less than 2 degrees, but it is possible to detect θ_p of 4 and 6 degrees, for example.

Finally, in Figure 11 we show the HMS and SOS apertures on the same scale viewed face-on. While the HMS vertical acceptance is nearly flat, its horizontal acceptance has a gaussian-like profile for long targets. For a 15 cm target the FWHM of ϕ is 55 mrad, and we have denoted this with dashed lines. If an electron is detected in the HMS at the

circled numbers 1, 2, or 3, and the produced Δ mass is 1232 MeV/c^2, then the corresponding virtual photon vectors 1, 2, and 3 will lie along the thin vertical line in the middle of the SOS acceptance. Here we have taken as an example setting 2 from our kinematics. As W varies, the locus shifts from the center of the SOS. Simulations suggest that the acceptance does not change rapidly; this is obviously due to the huge horizontal acceptance of the SOS. At this setting the usable acceptance in W is very roughly 80 MeV.

Because A_e is proportional to $\sin\phi$, and the HMS-SOS spectrometer accepts a large range of ϕ, we must weight each accepted event by $\sin\phi$ in order to properly determine the equivalent counts for determining the statistical error. At small laboratory angles, where essentially the entire range of ϕ is accepted, the average weight tends toward $2/\pi \simeq .637$. At large laboratory angles, where only values of ϕ near 90 degrees are accepted, the weight approaches 1. The actual values from the simulation are found in the Tables 7 and 8 below for the case of Δ's centered on the SOS and Δ's off-center by 1.5 degrees, respectively. In the off-center case, the mean value of $\sin\phi$ drops significantly at larger out of plane angles. Happily, this effect is offset by increasing acceptance, so for $\theta_p = 4$ degrees the fudge factor is similar in the two cases. The 'fudge factor' multiplies the acquired average counts/bin to give the true effective counts/bin. We will multiply the reciprocal of the fudge factor by the naive number of events needed in order to get the total number of events required.

Table 7: Acceptance for out-of-plane laboratory angles. The tagged Δ locus is centered in the SOS acceptance. The 'fudge factor' multiplies the acquired average counts/bin to give the true effective counts/bin.

θ_p^{LAB}	Prob.	Relative Acceptance	Acceptance Correction	$\sin\phi$ Weight	Fudge Factor
0.5	0.1323	1.000	1.59	.637	1.01
1.0	0.1323	1.000	1.59	.637	1.01
1.5	0.1323	1.000	1.59	.637	1.01
2.0	0.1305	0.986	1.57	.637	1.00
2.5	0.1249	0.944	1.50	.619	.929
3.0	0.1179	0.891	1.42	.603	.856
3.5	0.08987	0.679	1.08	.690	.745
4.0	0.05565	0.420	.668	.810	.541
4.5	0.03727	0.281	.447	.861	.385
5.0	0.02448	0.185	.294	.891	.262
5.5	0.01510	0.114	.181	.909	.165
6.0	0.00745	0.056	.089	.917	.082

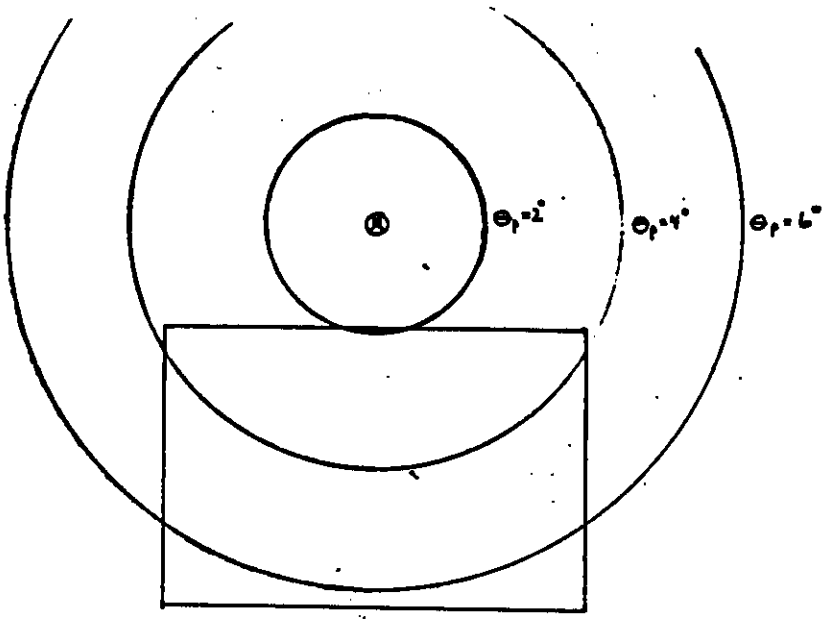

Figure 10: Looking along the direction of the virtual photon.

Table 8: Acceptance for out-of-plane laboratory angles. The virtual photon locus is 1.5 degrees off center in the SOS acceptance.

θ_p^{LAB}	Prob.	Relative Acceptance	Acceptance Correction	$\sin\phi$ Weight	Fudge Factor
0.5	0.1389	1.000	1.67	.637	1.06
1.0	0.1389	1.000	1.67	.637	1.06
1.5	0.1389	1.000	1.67	.637	1.06
2.0	0.1230	0.885	1.48	.686	1.02
2.5	0.0999	0.719	1.20	.707	.848
3.0	0.0856	0.616	1.03	.691	.712
3.5	0.0747	0.537	.897	.665	.597
4.0	0.0655	0.471	.786	.635	.499
4.5	0.0575	0.414	.690	.601	.415
5.0	0.0415	0.298	.498	.659	.328
5.5	0.0230	0.165	.276	.766	.211
6.0	0.0124	0.089	.149	.794	.118

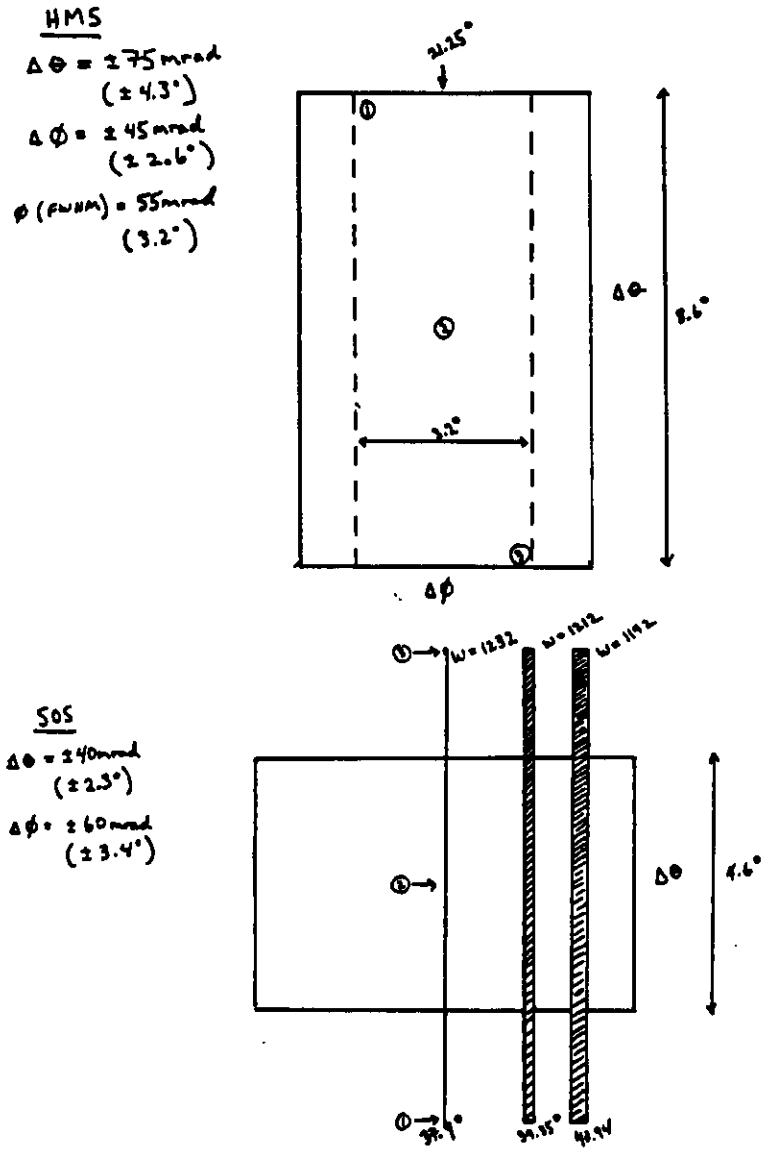

Figure 11: HMS and SOS angular acceptance viewed face-on. Magic kinematics cause the very narrow locus of virtual photon directions for fixed W.

D All About Rates

The HMS target related rates for the kinematic settings in this proposal are found in Table 9. All singles rates calculations were done using the codes of O'Connell and Lightbody. [23] The HMS is able to view a 10 cm long projected target length with good acceptance. Therefore for HMS angles less than about 42 degrees, the HMS will view the entire target length of 15 cm LH_2 including the Aluminum endcaps. Rates due to the endcaps have been neglected.

Table 9: Various rates in the HMS. Effective target length is 15 cm. Triggers are due to electrons only.

Setting	Current (μA)	e^- $d^2\sigma/d\Omega dP$ $\mu b/(srMeV/c)$	π^- $d^2\sigma/d\Omega dP$ $\mu b/(srMeV/c)$	π^-/e^-	Total HMS (MHz)	HMS Trigger (MHz)
1	25	$.187 \cdot 10^{-2}$	$.331 \cdot 10^{-4}$	.018	.465	.458
2	50	$.127 \cdot 10^{-2}$	$.113 \cdot 10^{-3}$	.089	.460	.417
3	50	$.488 \cdot 10^{-3}$	$.251 \cdot 10^{-3}$	.51	.189	.125
4	15	$.245 \cdot 10^{-2}$	$.197 \cdot 10^{-2}$	.008	.522	.510
5	20	$.635 \cdot 10^{-2}$	$.683 \cdot 10^{-4}$	.011	1.13	1.12
6	15	$.185 \cdot 10^{-2}$	$.116 \cdot 10^{-4}$	.006	.399	.387

The SOS target related rates for the six kinematic settings are found in Table 10. The SOS is able to view only a 5 cm long projected target length with good acceptance. At the SOS angles here, the effective target length is approximately 10 cm. Note that the SOS acceptance excludes the endcaps, so these will make no contribution to the real coincidence rate. The low SOS rates are a final advantage of our chosen kinematics; these angles place the SOS as far from the beamline as is possible.

Table 10: Various rates in the SOS. Effective target length is 10 cm. Triggers are due to protons only.

Setting	Current (μA)	p $d^2\sigma/d\Omega dP$ $\mu b/(srMeV/c)$	π^+ $d^2\sigma/d\Omega dP$ $\mu b/(srMeV/c)$	π^+/p	Total SOS (MHz)	SOS Trigger (MHz)
1	25	$.486 \cdot 10^{-3}$	$.679 \cdot 10^{-3}$	1.4	.172	.070
2	50	$.355 \cdot 10^{-3}$	$.443 \cdot 10^{-3}$	1.2	.251	.111
3	50	$.288 \cdot 10^{-3}$	$.319 \cdot 10^{-3}$	1.1	.209	.098
4	15	$.424 \cdot 10^{-3}$	$.417 \cdot 10^{-3}$	.98	.087	.044
5	20	$.293 \cdot 10^{-3}$	$.285 \cdot 10^{-3}$	.97	.086	.044
6	15	$.660 \cdot 10^{-3}$	$.476 \cdot 10^{-3}$	.72	.105	.063

In Table 11 are the random coincidence rates for each kinematic setting based on the previously discussed rates. The on-line coincidence window will be 10 ns, but this will be reduced to 2ns in the first offline pass with software mean-timing. The random rate can be further reduced offline by demanding that the SOS and HMS vertices coincide to within the vertex resolution and also by cuts on the mass of the reconstructed π^0. These software cuts are expected to increase the reals/randoms ratio by another factor of $1{\cdot}10^2$.

Table 11: Random coincidence rates between the HMS and SOS with online (10ns) and offline (2ns, first pass) timing windows.

No.	Randoms On-line	Randoms Off-line	Reals	Reals/Randoms On-line	Reals/Randoms Off-line	Total On-line
1	321	64	604	1.9	9.5	925
2	463	93	432	.93	4.7	895
3	123	41	229	1.9	9.5	352
4	224	45	797	3.6	18.	1021
5	488	98	309	.63	3.2	797
6	244	49	738	3.0	15.0	982

E Discussion of errors

A conservative estimate of the beam polarization which will be available near startup is 50%. For an A_e value of .03, and a beam polarization uncertainty of $\pm 5\%$, the error in the A_e measurement due to polarization uncertainties alone is $\pm .0015$. By striving for roughly similar statistical errors ($1.5 \cdot 10^6$ counts), we intend to achieve relative errors dA/A per bin of about 7.5%. (See Table 12.) If the beam polarization is increased to 75% the counts needed per angle bin decreases by roughly a factor of 2.

Table 12: Errors in A_e due to counting statistics and uncertainty in the beam polarization. We consider $A_e = .03$ as a typical predicted value. The variable ϵ is the expected counts asymmetry, or $(N^+ - N^-)/(N^+ + N^-)$.

Pol_{beam}	δPol_{beam}	ϵ	Total Counts	$\delta A_e^{stat.}$	$\delta A_e^{pol.}$	$\delta A_e^{e.+p.}$	dA_e/A_e
.5	.025	.015	$1.5 \cdot 10^6$	.00163	.00150	.00222	.0739
.75	.0375	.0225	$7 \cdot 10^5$	.00159	.00150	.00219	.0729

In measuring such a small asymmetry we will obviously be in big trouble if the background of irreducible random coincidences has a large value of A_e. We expect that the random coincidences will be dominated by protons in the SOS from Δ resonance decays and electrons in the HMS from the elastic radiative tail or uncorrelated Δ production. Fortunately, A_e vanishes for elastic scattering, and we are already painfully aware that A_e from Δ decay is small. Furthermore, as discussed in Appendix D, after all software cuts we expect that the reals/randoms ratio will be of order 10^2 to 10^3. It is also true that A_e need not vanish in quasi-free knockout reactions, but the SOS will not view the endcaps and the concentration of deuterium in natural hydrogen is insignificant ($1.5 \cdot 10^{-4}$). For these reasons we have not investigated the effects of backgrounds in the error analysis.

Finite energy and angle resolution determines our resolution in Q^2 which essentially defines our minimum useful binsize. A_e is not predicted to change change significantly over the scale of our Q^2 resolution, so this is not likely to affect our fit to extract values for $A_e(Q^2) = .3$ and .4 $(GeV/c)^2$. Table 13 shows our Q^2 resolution for each setting. However, due to our limited knowledge of the *absolute* incident and scattered energies and angles, we do not know the *absolute* value for the mean of Q^2. This introduces an error of size $\delta Q^2(dA_e/dQ^2)$. The estimate for the derivative (.2) is based on the predicted change in A_e for $G_C = 0.0$ from $Q^2 = .3$ to .4 . The size of this error is somewhat less than our A_e error goal of 7.5%, but it makes a significant contribution at a Q^2 of .4 (see last column). These results suggest that we should make every effort to keep the Q^2 indeterminacy under control and that we must reduce the polarization uncertainty from 5% to better than 4%. Since our original polarization uncertainty assumption was conservative, we should be able to meet these demands.

Table 13: Systematic error in A_e due to indeterminacy in the mean of Q^2. An A_e value of .03 was assumed.

Q^2	.075*A_e	$\delta(Q^2)$	$\delta^2(dA_e/dQ^2)$	$dA_e^{Q^2}/A_e$	dA_e^{tot}/A_e
.3	.00225	.0032	.00064	.021	.077
.4	.00225	.0075	.0015	.050	.088

References

[1] N. Isgur, G. Karl, and R. Koniuk, Phys. Rev. **D25** (1982) 2394.

[2] C. Becchi and G. Morpurgo, Phys. Lett. **17** (1965) 352.

[3] J. Bienkowska and Z. Dziembowski, Phys. Rev. Lett. **59** (1987) 624.

[4] R.D. Viollier, S.A. Chin, and A.K. Kerman, Nucl. Phys. **A407** (1983) 269.

[5] M.V.N. Murphy and R.K. Bhaduri, Phys. Rev. Lett. **54** (1985) 745.

[6] N. Isgur and G. Karl, Phys. Rev. **D18** (1978) 4187, and **D19** (1979) 2653.

[7] R. Davidson *et al.*, Phys. Rev. Lett. **56** (1986) 804.

[8] M. Bourdeau and N. Mukhopadhyay, Phys. Rev. Lett. **58** (1987) 976.

[9] R.M. Davidson and N. Mukhopadhyay, Phys. Rev. **D42** (1990) 20.

[10] R.M. Davidson *et al.*, Phys. Rev. **D43** (1991) 71.

[11] J. Jourdan *et al.*, CEBAF proposal PR-89-006.

[12] V. Burkert and R. Minehart *et al.*, CEBAF proposal PR-89-037.

[13] V. Burkert and R. Minehart *et al.*, CEBAF proposal PR-89-042.

[14] S. Nozawa and T.-S. H. Lee, Nucl. Phys. **A513** (1990), 511-542.

[15] S. Nozawa and T.-S. H. Lee, Nucl. Phys. **A513** (1990), 543-556.

[16] J.M. Laget, Nucl. Phys. **A481** (1988), 765-780.

[17] A. Raskin and T. Donnelly, Ann. Phys. **191** (1989) 78.

[18] C. Papanicolas, Bates proposal 86-13, and revision.

[19] Costas Papanicolas, private communication.

[20] Larry Cardman, private communication.

[21] P. Ulmer, private communication.

[22] Donal Day and Nicholas Phillips, 'Cerenkov Detector Design', unpublished.

[23] J. O'Connell and J. Lightbody, Comp. in Phys. May-June (1988) **57**.

[24] Satoshi Nozawa, private communication.

[25] R. Siddle *et al.*, Nucl. Phys. **B35** (1971) 93.